

# UC Davis

## UC Davis Previously Published Works

### Title

The potassium channel KCa3.1 constitutes a pharmacological target for neuroinflammation associated with ischemia/reperfusion stroke

### Permalink

<https://escholarship.org/uc/item/0339b8qr>

### Journal

Cerebrovascular and Brain Metabolism Reviews, 36(12)

### ISSN

1040-8827

### Authors

Chen, Yi-Je  
Nguyen, Hai M  
Maezawa, Izumi  
[et al.](#)

### Publication Date

2016-12-01

### DOI

10.1177/0271678x15611434

Peer reviewed

**The potassium channel KCa3.1 constitutes a pharmacological target for  
neuroinflammation associated with ischemia/reperfusion stroke**

Abbreviated Title: KCa3.1 channels in stroke

Yi-Je Chen<sup>1,2</sup>, Hai M. Nguyen<sup>1</sup>, Izumi Maezawa<sup>3,4</sup>, Eva M. Grössinger<sup>1</sup>, April Lourdes Garing<sup>1</sup>,  
Ralf Köhler<sup>5</sup>, Lee-Way Jin<sup>3,4</sup>, and Heike Wulff<sup>1</sup>

<sup>1</sup>*Department of Pharmacology, <sup>2</sup>Microsurgery Core, University of California, Davis, CA 95616, USA*

<sup>3</sup>*Department of Pathology and Laboratory Medicine, <sup>4</sup>M.I.N.D. Institute, University of California, Davis, Sacramento, CA 95817, USA*

<sup>5</sup>*Aragon Institute of Health Sciences / IIS and ARAID, Zaragoza, E-50009, Spain*

**Correspondence:** Heike Wulff, Department of Pharmacology, Genome and Biomedical Sciences Facility, Room 3502, 451 Health Sciences Drive, University of California, Davis, Davis, CA 95616; phone: 530-754-6136; email: [hwulff@ucdavis.edu](mailto:hwulff@ucdavis.edu)

**Acknowledgement:** This work was supported by a National Institute of General Medicine Award GM076063 to H.W., a National Institute of Aging Award AG043788 to I.M., and the Alzheimer's Disease Center at the University of California Davis funded by NIH/NIA (P30 AG10129). We are grateful for the technical support, products and services provided to our research by the Mouse Biology Program ([www.mousebiology.org](http://www.mousebiology.org)) at the University of California Davis.

**ABSTRACT**

Activated microglia/macrophages significantly contribute to the secondary inflammatory damage in ischemic stroke. Cultured neonatal microglia express the K<sup>+</sup> channels Kv1.3 and KCa3.1, both of which have been reported to be involved in microglia-mediated neuronal killing, oxidative burst and cytokine production. However, it is questionable whether neonatal cultures accurately reflect the K<sup>+</sup> channel expression of activated microglia in the adult brain. We here subjected mice to middle cerebral artery occlusion (MCAO) with 8 days of reperfusion and patch-clamped acutely isolated microglia/macrophages. Microglia from the infarcted area exhibited higher densities of K<sup>+</sup> currents with the biophysical and pharmacological properties of Kv1.3, KCa3.1 and Kir2.1 than microglia from non-infarcted control brains. Similarly, immunohistochemistry on human infarcts showed strong Kv1.3 and KCa3.1 immunoreactivity on activated microglia/macrophages. We next investigated the effect of genetic deletion and pharmacological blockade of KCa3.1 in reversible MCAO. *KCa3.1*<sup>-/-</sup> mice and wild-type mice treated with the KCa3.1 blocker TRAM-34 exhibited significantly smaller infarct areas on day-8 after MCAO and improved neurological deficit. Both manipulations reduced microglia/macrophage activation and brain cytokine levels. Our findings suggest KCa3.1 as a pharmacological target for ischemic stroke. Of potential clinical relevance is that KCa3.1 blockade is still effective when initiated 12 hours after the insult.

**Keywords:** KCa3.1, microglia activation, middle cerebral artery occlusion, potassium channel, TRAM-34

## INTRODUCTION

Inflammation significantly contributes to the pathophysiology of stroke, one of the leading causes of death in industrialized countries. Within hours after an ischemic or hemorrhagic insult, microglia, which continuously survey the CNS parenchyma,<sup>1</sup> become activated by “danger signals” such as ATP released from dying neurons, retract their branched processes, round up, and transform into “reactive” microglia, which produce IL-1 $\beta$ , TNF- $\alpha$ , reactive oxygen species, and nitric oxide, and contribute to the secondary expansion of the infarct.<sup>2, 3</sup> In addition to activated microglia, which are often called “resident brain macrophages”, human and rodent infarcts also typically contain macrophages arising from infiltrating monocytes.<sup>3, 4</sup> While there is starting to be consensus about the fact that microglia in the intact adult brain are normally not renewed by bone-marrow derived progenitors,<sup>5</sup> monocyte-derived macrophages start invading the brain within roughly 10 hours after an insult and many studies have shown large numbers of CD45<sup>high</sup> monocyte-derived macrophages and CD45<sup>low/medium</sup> microglia-derived macrophages at 24 h or 48 h after an ischemic insult when using flow cytometry to distinguish between the cell types.

Based on its delayed time course modulation of inflammation has been proposed as a more realistic target for stroke therapy than acute neuroprotection, which has largely failed to show efficacy in humans.<sup>6</sup> Several anti-inflammatory or immunosuppressive therapies have entered clinical trials and have so far had mixed success. Approaches to prevent neutrophils from infiltrating the brain by blocking adhesion molecules with Hu-23F2G, an anti-CD11/CD18 integrin antibody, or with enlimomab, an anti-ICAM1 antibody, recently failed in Phase-III clinical trials,<sup>6</sup> while an open-label Phase-II study and a Phase-I dose-finding study have shown the tetracycline antibiotic minocycline to be safe<sup>7</sup> and potentially effective in acute ischemic stroke when given for 5 days after the insult.<sup>8</sup> These findings together with a large body of literature on minocycline’s effects on microglia/macrophages in various models of brain injury,<sup>7</sup> suggest that targeting microglia/macrophages might be beneficial in stroke and that other microglia/macrophage-targeted approaches should be evaluated.

The voltage-gated potassium channel Kv1.3 and the calcium-activated potassium channel KCa3.1 play important roles in microglia activation by modulating  $\text{Ca}^{2+}$  signaling, oxidative burst, cytokine production and microglia-mediated neuronal killing.<sup>9-11</sup> Both channels are also expressed in monocyte derived macrophages.<sup>12</sup> Similar to findings in T cells, where the roles of Kv1.3 and KCa3.1 have been studied in great detail, the channels regulate membrane potential and  $\text{Ca}^{2+}$  signaling in microglia and monocyte derived macrophages.<sup>12</sup> However, most previous studies have been performed with cultured neonatal mouse or rat microglia,<sup>13</sup> and it has been questioned whether these systems correctly represent microglia *in vivo*. Here we demonstrate that microglia/macrophages acutely isolated from the infarct area in mouse MCAO express Kir2.1, Kv1.3 and KCa3.1 channels. We hypothesized that KCa3.1 channels are mechanistically involved in microglia/macrophage-mediated neuronal damage and demonstrate that both genetic deletion and pharmacological inhibition of KCa3.1 reduce infarct area and improve neurological deficit by reducing microglia/macrophage-mediated neuronal killing and inflammatory cytokine production. These results significantly expand our previous findings in a rat model<sup>14</sup> by 1) validating KCa3.1 as a target in a second species; 2) providing genetic confirmation in *KCa3.1*<sup>-/-</sup> mice; and 3) illuminating the mechanisms of how KCa3.1 blockers exert beneficial effects in stroke.

## MATERIALS AND METHODS

### Middle Cerebral Artery Occlusion (MCAO) Surgery

This study was approved by the University of California, Davis, Animal Use and Care Committee and conducted in accordance with the United States Public Health Service Policy on the Humane Care and Use of Laboratory Animals and the Guide for the Care and Use of Laboratory Animals. Animal care was in accord with the National Institutes of Health Guidelines and ensured animal comfort. The study is in compliance with the ARRIVE guidelines. *KCa3.1*<sup>-/-</sup> mice<sup>15</sup> were re-derived onto the C57BL/6J background by the Mouse Biology Program at the University of California Davis, and were bred homozygously since June 2012. Male 12-week old wild-type C57BL/6J (Jackson Laboratory, Sacramento, CA) or *KCa3.1*<sup>-/-</sup> mice (Mouse Biology Program, UC Davis) were acclimatized to the new vivarium for 5 to 7 days before surgery. Animals were anesthetized using box induction with 5% isoflurane in medical grade oxygen and then maintained on 0.5 to 1.5% isoflurane via a facemask. To assure consistent and continuous reduction of cerebral blood flow (CBF) throughout the procedure, a Laser Doppler (Moor Instruments, Wilmington, DE) was used throughout the surgery. Reversible focal cerebral ischemia was then induced by occlusion of the left middle cerebral artery (MCA) as previously described for rats.<sup>14</sup> Briefly, the left common carotid artery was surgically exposed, the external carotid artery was ligated distally from the common carotid artery, and a silicone rubber-coated nylon monofilament with a tip diameter of  $0.21 \pm 0.02$  mm (Doccol Corp., Redlands, CA) was inserted into the external carotid artery and advanced into the internal carotid artery to block the origin of the MCA.<sup>14, 16</sup> The filament was kept in place for 60 min and then withdrawn to restore blood supply. The mice received subcutaneous Buprenex at 0.02 mg/kg every 12 h to limit post-surgical pain for 24 h after surgery. The survival rate was 85% in both wild-type and *KCa3.1*<sup>-/-</sup> mice. Sham surgeries were performed with identical blood vessel exposure and preparations. The filament was placed into the external carotid artery but not advanced into the internal carotid artery.

Starting 12 h after reperfusion animals started receiving either the vehicle miglyol 812 neutral oil (caprylic/capric triglyceride; Tradename Neobee M5<sup>®</sup>, Spectrum Chemicals, Gardena, CA) or TRAM-34 at 40 mg/kg every 12 h until sacrifice on day-8. TRAM-34 was synthesized in our laboratory as previously described.<sup>17</sup> Neurological deficits were scored according to a 4-score test<sup>18</sup> and a tactile and/or proprioceptive limb-placing test<sup>19</sup> as previously described.<sup>14</sup>

### **Microglia/Macrophage Isolation**

Eight days after reperfusion MCAO mice were anesthetized with isoflurane and killed by cervical dislocation. Brains were removed quickly; the infarcted hemispheres were collected and kept in ice-cold Hank's balanced salt solution (HBSS) after removing cerebellum and brain stem. The brain tissue was chopped into small pieces with a sterilized blade and then centrifuged at 300 g for 2 min to remove the supernatant. Following digestion with enzyme mix 1 for 15 min and enzyme mix 2 for 10 min at 37°C, brain tissue was mechanically dissociated by pipetting up and down with 1 ml and 100 µl tips. The tissue suspension was centrifuged at 300 g at 4°C for 10 min to spin down the cells. Magnetic microbeads conjugated to CD11b antibody were added to the cell suspension and microglia were isolated with the Miltenyi magnet according to the manufacturer's protocol (CD11b microglia MicroBeads kit, Miltenyi Biotec Inc.). As a control for activated microglia, we also isolated microglia from the hippocampus of 12-week old wild-type mice 48 h after intracerebroventricular lipopolysaccharide (LPS) injection (8 µg per mouse). Due to the close proximity of the hippocampus to the ventricular system, the isolated microglia would show maximal Toll-like receptor 4-induced activation.

### **Electrophysiology**

Acutely isolated microglia were plated on poly-L-lysine-coated glass coverslips immediately after isolation and then incubated at 37°C for 10 minutes before electrophysiological recordings. Overall, the isolation procedure lasted 90 min from the removal of the brains until the microglia were on the

microscope stage ready to be patch-clamped. Currents were recorded using the whole-cell configuration of the patch-clamp technique at room temperature with an EPC-10 HEKA amplifier. External normal Ringer solution contained 160 mM NaCl<sub>2</sub>, 4.5 mM KCl, 2 mM CaCl<sub>2</sub>, 1 mM MgCl<sub>2</sub>, 10 mM HEPES, pH 7.4, 300 mOsm. Patch pipettes were filled with an internal solution containing 145 mM K<sup>+</sup> aspartate, 2 mM MgCl<sub>2</sub>, 10 mM HEPES, 10 mM K<sub>2</sub>EGTA, and 8.5 mM CaCl<sub>2</sub> (1 μM free Ca<sup>2+</sup>), pH 7.2, 290 mOsm. K<sup>+</sup> currents were elicited with voltage ramps from -120 to 40 mV of 200-ms duration applied every 10 s. Access resistance was monitored continuously and no RS compensation was used since access resistances typically stayed below 10 MΩ. KCa3.1 conductances were calculated from the slope of the TRAM-34-sensitive K<sub>Ca</sub> current between -80 and -75 mV, where KCa3.1 currents are not “contaminated” by Kv1.3 (which activates at voltages more positive than -40 mV) or inward rectifier K<sup>+</sup> currents (which are appreciable at voltages more negative than -80 mV). Inward rectifier (K<sub>ir</sub>) currents were measured as peak inward currents at -120 mV and Kv1.3 currents were measured as TRAM-34-insensitive, use-dependent outward currents at +40 mV from the same voltage ramp protocol. In some experiments Kv currents were recorded with a KF-based Ca<sup>2+</sup>-free internal solution and elicited by voltage steps from -80 to +40 mV as previously described.<sup>20</sup> Cell capacitance, a direct measurement of cell surface area, was continuously monitored during recordings. KCa3.1 current density was determined by dividing the TRAM-34-sensitive slope conductance by the cell capacitance. K<sub>ir</sub> and Kv1.3 current densities were determined by dividing their current amplitudes at -120 mV (K<sub>ir</sub>) or +40 mV (Kv1.3) by the cell capacitance. The KCa3.1 blocker TRAM-34, and the Kv1.3 blockers PAP-1 and ShK-L5 were synthesized as previously described.<sup>17, 21</sup>

### **Immunohistochemistry (IHC) and Immunofluorescence (IF) Staining**

Paraffin-embedded human brain sections from eight cases containing infarcts varying in age from 10 days to 8 weeks were obtained from the Alzheimer’s Disease Center at the University of California Davis. The tissue procurement was approved by the Institutional Review Board of the University of California, Davis. Informed consent to share research tissue after death was obtained from all patients or a

representative prior to their death. The age of the infarct in each case was based on corroborating clinical history and pathological evaluation by an experienced neuropathologist (L.-W. J.). Sections were dewaxed with xylene, rehydrated through an alcohol gradient, and heated with 10 mM Na citrate (pH 6.0) in a microwave for 15 min to retrieve antigenic determinants. After treatment with 1% H<sub>2</sub>O<sub>2</sub> to inactivate endogenous peroxidase activity and blocking with 5% goat serum, sections were incubated overnight at 4°C with the primary antibody in phosphate-buffered saline with 2% goat serum. KCa3.1 was stained for with a rabbit polyclonal anti-KCa3.1 antibody (1:3000, AV35098, Sigma-Aldrich) and Kv1.3 with a mouse monoclonal anti-human Kv1.3 antibody (1:100; 1D8, AbD Serotec). The specificity of the antibodies has been previously described.<sup>22</sup> Bound primary antibodies were detected with a biotinylated goat anti-rabbit IgG secondary antibody for KCa3.1 and a biotinylated donkey anti-mouse IgG secondary antibody for Kv1.3 (both 1:500, Jackson ImmunoResearch, West Grove, PA) followed by a horseradish peroxidase-conjugated avidin complex (Vectastain Elite ABC Kit, Vector Laboratories, Burlingame, CA). Peroxidase activity was visualized with 3,3'-diaminobenzidine (DAB Substrate Kit for Peroxidase, Vector Laboratories). Sections were counterstained with hematoxylin (Fisher, Pittsburg, PA), dehydrated and mounted with Permount (Fisher).

For the human IF images in Figure 3B and 3D, Kv1.3 was stained for with a rabbit polyclonal anti-Kv1.3 antibody (1:100, APC-002, Alomone, Israel), KCa3.1 with the AV35098 antibody and microglia/macrophages with a mouse monoclonal anti-human macrophage antibody (1:100, MCA874G, AbD Serotect, Raleigh, NC). For the mouse IF images in Figure 4, KCa3.1 was stained with the AV35098 antibody (1:3000) and microglia/macrophages with a rat monoclonal anti-mouse CD68 antibody (1:200, FA-11, AbD Serotec). Bound primary antibodies were detected by Alexa Fluor®546-conjugated or Alexa Fluor®647-conjugated secondary antibodies (A-11010, A-21235 or A-21247, 1:500, Life Technologies). Sections were mounted in Fluoromount-G (SouthernBiotech) with DAPI and imaged with a Zeiss LSM-510 confocal microscope. For the IHC staining shown in Figure 5 mouse brain sections were dewaxed, subjected to antigen retrieval and blocked as described above. The following primary antibodies were used: NeuN (1:1,000; A60, Millipore, Billerica, MA), Iba-1 (1:200; 019-19741, Wako

Chemicals, VA). Bound primary antibodies were detected with biotinylated secondary antibodies, visualized with DAB and counterstained as described above for the human brain sections.

### **Assessment of Infarct Area**

Mice were killed with an overdose of isoflurane and brains were quickly removed and sectioned into four 2-mm thick coronal slices starting from the frontal pole. Slices were then fixed in 10% buffer formalin overnight, embedded in paraffin and sectioned at 5  $\mu$ m. All sections were stained with anti-NeuN antibody for neuron viability as described above and scanned by an automated microscopy system (Eclipse Ni-E, Tokyo, Japan) with a 10X objective lens. The resulting jpg images from all sections were analyzed in Adobe Photoshop CS3 for infarct area using the Magnetic Lasso tool to outline the area (NeuN negative area) and the Histogram tool to determine the number of pixels in the respective area. Percent infarct for each slice was calculated as: [pixels in ipsilateral side/pixels in whole control hemisphere] x 100. Percentage of total infarct area in the whole hemisphere was calculated as: [summation of pixels in infarct from 4 slices/summation of pixels in whole control hemisphere from 4 slices] x 100. We evaluated infarct area by NeuN staining because NeuN produces better contrast than H&E on heavily formalin fixed aged infarcts and is also more amendable to pixel based analysis on an automated microscope system.

### **Assessment of Microglia/Macrophage Activation/Infiltration**

Sections consecutive to the NeuN-stained sections in Figure 5 from the center of the infarct (4 mm and 6 mm from the frontal pole) from all animals were staining with anti-Iba-1 antibody to determine microglia/macrophage activation and infiltration. Images of whole sections were acquired as jpg images by an automated microscopy system as described above. The number of Iba-1-positive (dark brown) cells in the ipsilateral and contralateral hemisphere were analyzed by Image J. Briefly, the whole brain image was cropped to generate two images, one of each hemisphere. After converting the images to binary, the “Threshold”, “Watershed”, and ”Analyze Particles” were adjusted to properly highlight and

automatically count the number of Iba-1 positive cells. The intensity of microglia/macrophage infiltration is presented as the ratio of Iba-1 positive cells in the ipsilateral hemisphere to the contralateral hemisphere.

### **Analysis of Brain Cytokines**

Cytokines (IL-1 $\beta$ , IL-4, IL-6, IL-10, IFN- $\gamma$ , TNF- $\alpha$ ), BDNF and TGF- $\beta$ 1 in brain extract were analyzed with Millipore Milliplex mouse magnetic bead kits and a Luminex 200TM reader according to the manufacturer's instructions. Mice from different treatment groups were killed with an overdose of isoflurane on day-8 after MCAO. Brains were collected and snap frozen with liquid nitrogen. Brain extracts were prepared as described.<sup>23</sup> Briefly, single hemispheres were trimmed, weighed and homogenized with a Polytron bench top homogenizer in a 10X volume of extraction buffer. Following centrifuged (1,000 g) for 10 min at 4°C, the supernatant was collected and centrifuged a second time (20,000 g for 40 min at 4°C) to remove any remaining debris. The supernatant was collected and analyzed for protein (assayed by the bicinchoninic (BCA) procedure) and cytokine content. Equal volumes of brain extract were loaded for measurements and the results were normalized to pg/mg of total protein content in each sample.

### **Hippocampal slice culture and hypoxia treatment**

Hippocampal slice cultures (400  $\mu$ m thick) were prepared from 7-day-old C57BL/6J mice as described.<sup>24</sup> After 3 days of culture *in vitro*, medium was changed to a hypoxic/hypoglycemic medium (75% Neurobasal, 25% HBSS, 1% L-glutamine, bubbled with 99.4% nitrogen). Slices were placed in a hypoxia incubation chamber (Stemcell Technologies) and nitrogen gas was flown into the chamber (20 L/min, 4 min) according to the vender's instruction, followed by incubation at 37° for 1 h. The culture medium was replaced by normal culture medium containing glucose and slices were placed in a tissue culture incubator (95%O<sub>2</sub>/5%CO<sub>2</sub>). After 2 h of culture, TRAM-34 (1  $\mu$ M) and doxycycline (1  $\mu$ M) were added

and slices were cultured for 3 days. Slices were then fixed in 4% paraformaldehyde and stained with anti-Iba1 (1:400; Wako Chemical) and anti-NeuN (1:400; Chemicon) overnight at 4°C followed by a secondary Alexa488-conjugated anti-mouse or Alexa568-conjugated anti-rabbit antibody (1:700; Molecular Probes). Immunostained slices were observed using a Nikon Eclipse E600 microscope and photographed by a digital camera (SPOT RTke; SPOT Diagnostics, Sterling Heights, MI). Culture medium (collected after 3 days of culture) was analyzed for TNF- $\alpha$  and IL-1 $\beta$  by Sandwich ELISA according to the manufacturer's instruction (R&D Systems).

### **Statistical Analysis**

Statistical analysis of infarct area, neurological deficit scoring and IHC were performed with one-way analysis of variance (ANOVA; Origin software) followed by *post-hoc* pair-wise comparison of the different groups using Tukey's method, also referred to as honestly significant difference test, as recommended by Schlattmann and Dirnagl for MCAO studies.<sup>25</sup> Shown are mean  $\pm$  S.E.M.  $p < 0.05$  was used as the level of significance. \* =  $p < 0.05$ , \*\* =  $p < 0.01$ , \*\*\* =  $p < 0.001$ . Electrophysiological data are presented as mean  $\pm$  S.D. and statistical significance was determined by Student's *t*-test.

## RESULTS

### **Acutely Isolated Microglia/Macrophages from the Brains of Mice Subjected to MCAO with 8 Days of Reperfusion Exhibit Increased $K^+$ Channel Function**

To investigate the expression and pathomechanistic roles of  $K^+$  channels in microglia/macrophages in ischemic stroke, we subjected adult mice to 60-min of MCAO followed by reperfusion. Eight days after MCAO, brains were removed, the infarct area dissected, and microglia/macrophages isolated with magnetic beads (Figure 1). The isolate cells were then used immediately for immunostaining or electrophysiology. Confocal double immunofluorescence showed strong punctate staining for Kv1.3 and KCa3.1 on CD11b-positive cells from the infarcted area of MCAO brains (Figure 1), while whole-cell patch-clamp revealed increased functional expression of Kv, KCa and Kir currents following MCAO (Figure 2). Kv channel density was very low or often barely detectable in microglia isolated from normal, non-ischemic brains or microglia from the contralateral side after MCAO (Figure 2A). In contrast, microglia isolated from the infarcted area after MCAO or from the hippocampus of adult mice 48 hours after intracerebroventricular LPS injection were clearly activated based on their increased cell size (measured as capacity) and showed roughly 5-fold larger Kv currents (Figure 2A), which seemed to be predominantly carried by Kv1.3 based on their use-dependence and sensitivity to the specific Kv1.3 blockers PAP-1 and ShK-L5 (Figure 2B). MCAO and LPS injection also increased expression of a  $Ca^{2+}$ -activated  $K^+$  channel (Figure 2C), which, based on its sensitivity to TRAM-34 was identified as KCa3.1 (Figure 2D). Interestingly, KCa3.1 currents were also slightly increased in microglia isolated from the contralateral side after MCAO probably reflecting a general, heightened state of inflammation and microglia activation in the entire brain following a large stroke. We further observed increased expression of a  $Ba^{2+}$ -sensitive (data not shown) Kir channel following MCAO in both the contralateral and the infarcted hemisphere but not following intracerebroventricular LPS injection (Figure 2E and 2F).

### **Immunohistochemistry Demonstrates Kv1.3 and KCa3.1 Expression on Microglia/Macrophages in Human Infarcts**

In order to provide some human target validation and test whether the channels we had observed by electrophysiology in mice are also present in human infarcts, we performed immunohistochemical experiments on sections from eight cases with ischemic infarcts varying in age from 10 days to 8 weeks. Invariably, the infarcted areas showed intense KCa3.1 staining (Figure 3A), which, on closer examination, localized to activated microglia/macrophages (M) and vascular endothelial cells (E), where KCa3.1 is expressed and involved in fluid movement<sup>14</sup> and endothelium-derived hyperpolarization.<sup>15, 26</sup> Immunofluorescence confirmed KCa3.1 expression on amoeboid-shaped microglia/macrophages (Figure 3B). We further stained brain sections for Kv1.3 and observed similar intense Kv1.3 staining in the infarct areas, localized to microglia/macrophages (Figure 3C and 3D). In contrast to KCa3.1, Kv1.3 was not expressed on endothelial cells (Figure 3C), as expected from its expression pattern.<sup>27</sup> No KCa3.1 or Kv1.3 immunoreactivity was observed in non-infarcted areas, with the exception of KCa3.1 on vascular endothelium and perivascular macrophages. The staining results were consistent among the eight cases, supporting enhanced expression of KCa3.1 and Kv1.3 in microglia/macrophages in human ischemic infarcts.

Based on the K<sup>+</sup> channel expression pattern in microglia/macrophages isolated from adult mice following ischemic stroke or observed in humans by immunohistochemistry, we decided to concentrate on KCa3.1 in this paper. The role of Kv1.3 in ischemic stroke deserves a separate study while Kir2.1 is not a particularly attractive pharmacological target for the suppression of post-stroke inflammation in our opinion because the channel has no well-characterized inhibitors other than Ba<sup>2+</sup> and plays vital roles in the heart.<sup>28</sup>

### **Genetic KCa3.1 Deletion and Pharmacological Blockade Reduce Infarct Area and Improve Neurological Deficit in Middle Cerebral Artery Occlusion with Reperfusion**

In order to evaluate the effects of KCa3.1 deficiency or pharmacological blockade on the pathology of experimental ischemic stroke we subjected wild-type and *KCa3.1*<sup>-/-</sup> mice to reversible focal cerebral ischemia induced by 60-min occlusion of the left middle cerebral artery (MCA) according to the method of Zea Longa.<sup>16</sup> Five days after reperfusion confocal microscopy revealed activated CD68<sup>+</sup> microglia/macrophages in the infarct zone (Figure 4). In the *KCa3.1*<sup>-/-</sup> mice these CD68<sup>+</sup> cells lacked KCa3.1 staining (Figure 4A), while they exhibited strong KCa3.1 staining in wild-type animals (Figure 4B). Higher magnification showed that the stains clearly were on the same cells but did not co-localize (Figure 4C). This was to be expected because CD68 is a lysosomal protein while KCa3.1 is expressed on the plasma membrane and traffics through the endoplasmic reticulum.

After surgery, mice were scored daily for neurological deficit until sacrifice on day-8. Starting 12 hours after reperfusion mice were treated twice daily with either vehicle or our KCa3.1 blocker TRAM-34.<sup>17</sup> Pharmacological treatment was delayed for 12 hours in order to simulate possible clinical treatment conditions. As shown in Figure 5A, both *KCa3.1*<sup>-/-</sup> mice and TRAM-34 treated wild-type mice exhibited a significant reduction in infarct area as defined by NeuN-negativity. The mean infarct area was reduced from  $25.0 \pm 3.0\%$  in vehicle treated wild-type mice (n = 11) to  $12.6 \pm 2.4\%$  in vehicle treated *KCa3.1*<sup>-/-</sup> mice (n = 17, p = 0.0027) and to  $10.3 \pm 1.4\%$  in TRAM-34 treated wild-type mice (n = 11, p = 0.0002).

Since filament MCAO induces infarction not only in the major MCA territory, the lateral and parietal cortex, but also in the striatum, we used a combination of two tests, the 4- and the 14-score test<sup>19</sup> to evaluate mice in a blinded fashion for sensorimotor coordination every 24 h. In the 4-score test, where a normal mouse has a score of 0 for no deficit, all three groups of mice displayed a score of roughly 3 on their first evaluation 12 h after surgery (Figure 5B). While vehicle-treated wild-type mice only slowly improved to a score of 2 on postsurgical day-8, *KCa3.1*<sup>-/-</sup> mice started to show significant improvements beginning from day-1 and improved to an average score of 0.5 on day-8. TRAM-34 treatment in wild-type animals beginning 12 h after reperfusion (= after the first neurological evaluation) achieved a similar improvement trend but lacked behind the much more obvious improvement in the knockout mice. In the

more graded 14-score tactile and proprioceptive limp-placing test, in which a normal mouse typically scores 14, wild-type mice started with a severe impairment 12 h after the surgery (score ~1), improved to an average score of 5 by day-4 and then leveled off at this score and showed no further improvement until day-8 (Figure 5C). In contrast, *KCa3.1*<sup>-/-</sup> mice already showed a trend towards improvement on the first evaluation 12 h after the surgery, had a significantly better score on day-1 and improved to an average score of 9 on day-8. Wild-type mice treated with TRAM-34 starting from 12 h after the surgery initially performed similar to vehicle treated mice but started to show significant improvements beginning on day-5 and improved to an average score of 9 by day-8, similar to *KCa3.1*<sup>-/-</sup> mice (Figure 5C).

In order to test TRAM-34 for selectivity we further treated a group of *KCa3.1*<sup>-/-</sup> mice with 40 mg/kg TRAM-34 twice daily for 8 days following MCAO. As expected based on the absence of its molecular target, TRAM-34 treatment produced no additional reduction in NeuN-negative infarct area (KO: 12.6 ± 2.4%, n = 17; KO + TRAM-34: 7.8 ± 0.9%, n = 12; p = 0.127) or improvement in neurological deficit in the 4-score test on day-8 (KO: 0.5 ± 0.2, n = 17; KO + TRAM-34: 0.8 ± 0.2, n = 12; p = 0.177) or the 14-score test at day-8 (KO: 8.0 ± 0.6, n = 17; KO + TRAM-34: 7.9 ± 0.3, n = 12; p = 0.484; all values are means ± S.E.M.).

### **Genetic KCa3.1 Deletion and Pharmacological Blockade Reduce Microglia/Macrophage Activation/Infiltration and Inflammatory Cytokine Production**

In order to test our hypothesis that KCa3.1-deletion and pharmacological blockade reduce infarct area in the first week following an ischemic insult by reducing microglia activation and potentially also macrophage infiltration, we evaluated Iba-1-staining intensity in vehicle treated wild-type, *KCa3.1*<sup>-/-</sup> and TRAM-34 treated mice. Analysis of the ratio of Iba-1-positive cells in the ipsilateral versus the contralateral hemisphere in sections from the center of the infarct revealed a significant reduction in Iba-1-positive cells in both *KCa3.1*<sup>-/-</sup> mice and TRAM-34 treated wild-type mice on day-8 after MCAO (Figure 6A).

We further determined brain cytokine levels on day-8 after MCAO in the ipsi- and contralateral hemisphere from sham-operated animals as well as vehicle-treated wild-type mice, *KCa3.1*<sup>-/-</sup> mice and TRAM-34-treated mice subjected to MCAO (Figure 6B). As expected, MCAO significantly increased levels of the inflammatory cytokines, IL-1 $\beta$  and IFN- $\gamma$ , as well as the pleiotropic cytokine TGF- $\beta$ 1 in the ipsilateral hemisphere. IL-1 $\beta$  production was drastically reduced by KCa3.1-deletion and TRAM-34 blockade, while IFN- $\gamma$  and TGF- $\beta$ 1 were only clearly reduced by TRAM-34 treatment and showed a trend towards reduction in brain extracts from *KCa3.1*<sup>-/-</sup> mice. MCAO further mildly increased IL-4 and IL-10 concentrations in the ipsilateral side as well as levels of the brain-derived nerve growth factor (BDNF) in both the ipsi- and contralateral side on day-8. TRAM-34 treatment again significantly reduced the levels of all three proteins, while KCa3.1-knockout only showed a trend towards reduction (Figure 6B). We also tried to measure TNF- $\alpha$  and IL-6, but found that levels of both cytokines were below detection on day-8 after MCAO in our hands. Taken together, these findings demonstrate that KCa3.1 suppression reduces microglia/macrophage activation and infiltration as well as cytokine and growth factor production 8 days after MCAO.

### **TRAM-34 Increases Neuronal Survival and Reduces Microglia Activation in Organotypic Hippocampal Slices**

We further investigated the effect of KCa3.1 blockade on activated microglia in organotypic hippocampal slice cultures, a widely used model for examining the effect of hypoxia. Hippocampal slices reflect conditions in the brain in terms of microglia interactions with neurons and astrocytes but allow no additional monocytes to infiltrate from the blood. Exposure of hippocampal slices to hypoxia/aglycemia for 60 min resulted in strong microglia activation and a drastic reduction in surviving NeuN<sup>+</sup> neurons 3 days later as determined by Iba-1 and NeuN staining (Figure 7A and 7B). Treatment of slices with TRAM-34 (1  $\mu$ M) or the microglia inhibitor doxycycline (1  $\mu$ M) resulted in a significant increase in neuronal survival and a reduction in microglia activation and IL-1 $\beta$  production on day-3 (Figure 7B and

7C). We also analyzed TNF- $\alpha$  but did not see a significant increase in TNF- $\alpha$  following hypoxia exposure and no significant change in TNF- $\alpha$  levels in the slice culture medium by TRAM-34 or doxycycline treatment (data not shown). Since neither TRAM-34 nor doxycycline are directly neuroprotective,<sup>11</sup> these observations suggest that KCa3.1 blockers increase neuronal survival by reducing hypoxia-stimulated microglia-mediated neuronal killing, similar to our previous report that TRAM-34 can reduce oligomeric amyloid- $\beta$ -induced microglia-mediated neuronal killing in dissociated cultures and organotypic hippocampal slices.<sup>11</sup>

## DISCUSSION

Using classical suture MCAO with reperfusion in mice as a model for ischemic stroke, we here show that genetic deletion and pharmacological blockade of KCa3.1 significantly reduces infarct area and improves neurological deficit eight days after the insult. KCa3.1 blockade inhibits microglia/macrophage activation, and reduces brain levels of the cytokines IL-1 $\beta$ , IFN- $\gamma$  and TGF- $\beta$ 1. *In vitro* experiments with organotypic hippocampal slices exposed to hypoxia/hypoglycemia confirm that KCa3.1 blockade improves neuronal survival by reducing microglia activation and IL-1 $\beta$  production as effectively as the minocycline derivative doxycycline. These results considerably extend our previous findings in a rat model,<sup>14</sup> which solely relied on pharmacological evidence, and further support KCa3.1 as a potential therapeutic target for reducing inflammatory damage in stroke. We are now providing genetic target validation by demonstrating that *KCa3.1*<sup>-/-</sup> mice exhibit significantly reduced pathology after MCAO. We are further confirming the specificity of our pharmacological tool compound TRAM-34 by showing that it exerts no beneficial effects in *KCa3.1*<sup>-/-</sup> mice and are corroborating its efficacy and the validity of targeting KCa3.1 in focal ischemic stroke in a second species. Additionally, our current study further provides some human target validation by showing strong KCa3.1 immunoreactivity on microglia/macrophages in human infarcts.

We also investigated the K<sup>+</sup> channel expression profile of microglia/macrophages from the infarcted area by subjecting them to whole-cell patch-clamp experiments immediately after isolation. We performed these experiments because it has widely been questioned whether findings made with cultured neonatal microglia truly reflect the K<sup>+</sup> channel expression profile of microglia in the adult brain [For an exhaustive review of ion channel and transporter expression in microglia please see<sup>13</sup>]. We are of course not the first group to record from adult microglia. Previous recordings in acute mouse or rat brain slices showed small Kir currents under normal conditions and increased Kv channel expression following facial nerve axotomy<sup>29</sup> or 48-hours after MCAO<sup>30</sup>. However, our study is the first to investigate calcium-activated K<sup>+</sup> channels in adult microglia and to identify both the Kv and the KCa channel through their

biophysical and pharmacological properties as Kv1.3 and KCa3.1. By comparing CD11<sup>+</sup> cells isolated from normal brains and the non-infarcted and infarcted hemisphere after MCAO with cells isolated from the hippocampus following intracerebroventricular LPS injection, we show that ischemic stroke increases functional Kir2.1 and KCa3.1 expression in both the infarcted and the non-infarcted hemisphere and Kv1.3 expression in the infarcted hemisphere. Interestingly, *in vivo* LPS-stimulation also increases Kv1.3 and KCa3.1 expression, but unlike MCAO does not stimulate inward rectifier expression. These differences in expression between MCAO- and LPS-stimulated microglia and the varying K<sup>+</sup> channel profiles observed after MCAO (e.g. cells with large Kir2.1 versus cells with predominantly KCa3.1 or a combination of KCa3.1 and Kv1.3) suggest the presence of microglia in different activation and differentiation states such as M1 and M2. Potentially aligning K<sup>+</sup> channel expression with different microglia subtypes will warrant further investigation. For the purposes of the current study the electrophysiological experiments provide clear evidence for functional KCa3.1 expression on microglia acutely isolated from the infarct area.

Taken together with our previous study demonstrating a ~50% reduction in infarct area when the KCa3.1 blocker TRAM-34 was administered starting 12 hours after reperfusion in rats<sup>14</sup> our current data strongly validate KCa3.1 as a potential therapeutic target for reducing inflammation and preventing the secondary expansion of the infarct area in the first week after the insult. The target for TRAM-34 in our study were most likely KCa3.1 channels on CD11<sup>+</sup> macrophages, arising either from the activation and proliferation of brain resident microglia or from infiltrating bone marrow-derived monocytes, although we cannot completely exclude additional effects on activated T cells or peripheral macrophages. In all these cell types, KCa3.1 is involved in proliferation, migration and inflammatory cytokine production by regulating Ca<sup>2+</sup> signaling processes and membrane potential.<sup>12, 13</sup> However, our experiments comparing TRAM-34 and doxycycline in a setting where no monocyte derived macrophages or infiltrating T cells can be present (see organotypic slice cultures in Figure 7) certainly demonstrate that KCa3.1 blockers strongly inhibit microglia activation but of course cannot completely exclude that KCa3.1 inhibition alters microglial activation status following stroke via an indirect mechanism, secondary to neuro- or vasculo-

protection by affecting other cell types such as vascular endothelial cells (see below for discussion), neurons or T cells *in vivo*. A recent publication suggested that KCa3.1 might be involved in the slow afterhyperpolarization in hippocampal neurons.<sup>31</sup> However, if there is any similarity between the roles of the fast (KCa1.1 = BK), medium (KCa2 = SK) and slow afterhyperpolarization (KCa3.1 = IK) in terms of neuroprotection, then it would be highly unlikely that KCa3.1 inhibition would be neuroprotective by inhibiting the sAHP. Typically, compounds that enhance the AHP are neuroprotective, while blockers rather have the opposite effect. In this context we would also like to point out that we have previously tested TRAM-34 for neuroprotection and found that it could not protect hippocampal neurons from cell death induced by microglia conditioning medium, but that it was neuroprotective when conditioning medium from TRAM-34 treated microglia was used,<sup>11</sup> arguing for an effect on microglia and not neurons. We further cannot rule out that inhibition of T cell activation contributes to the effect of TRAM-34 *in vivo*, but while there are certainly T cells in the inflammatory infiltrate following ischemic stroke their role is far from clear and is sometimes referred to as the “the lymphocyte puzzle” in stroke<sup>3</sup>.

The findings in the KCa3.1<sup>-/-</sup> mice largely confirm the pharmacological results and both KCa3.1 deletion and pharmacological blockade produce similar improvements in neurological deficit scores and reductions in infarct area by day-8 after MCAO (Figure 5). However, KCa3.1<sup>-/-</sup> mice perform strikingly better early on in the neurological evaluations. One reason for this could be that we started TRAM-34 administration only after the first neurological evaluation, 12 hours after reperfusion, in order for the treatment regimen to be translationally relevant. It is therefore possible that the KCa3.1<sup>-/-</sup> mice exhibited reduced microglia/macrophage activation right from the beginning. However, given the delayed time course of microglia activation,<sup>32</sup> another very plausible reason for the improved performance of the KCa3.1<sup>-/-</sup> mice early after MCAO could be reduced edema formation. In addition to activated microglia and macrophages, KCa3.1 is also expressed on blood brain barrier endothelial cells, where it helps drive transcellular Na<sup>+</sup> transport by the Na-K-Cl cotransporter (NKCC) and the Na/H exchanger (NHE) in the first few hours after ischemic stroke when the blood brain barrier is still intact.<sup>33</sup> Using magnetic resonance spectroscopy and Na<sup>+</sup> imaging we recently demonstrated that TRAM-34 treatment started

immediately before induction of permanent MCAO in rats significantly delayed edema formation and brain Na<sup>+</sup> uptake.<sup>33</sup> These edema reducing effects of KCa3.1 inhibition are very likely responsible for the better outcomes of the KCa3.1 mice early after MCAO. It could of course also be argued that TRAM-34 was not optimally dosed in this study. However, we have previously performed extensive pharmacokinetic studies with TRAM-34. The compound shows good brain penetration ( $C_{brain}/C_{plasma} = 1.2$ ) and a 40 mg/kg dose produced total brain concentrations exceeding 1 μM for 8 h and 400 nM for 12 h in rats.<sup>14</sup> Similar or even better concentrations are attainable in mice where we found  $12.3 \pm 4.3$  μM TRAM-34 in the brain 4 h after intraperitoneal applications (n = 8, data not shown). Another observation that argues that TRAM-34 was dosed high enough is the fact that both KCa3.1 deletion and TRAM-34 administration had very similar effects on brain cytokine concentrations and both reduced IL-1β, IFN-γ, IL-4, and IL-10. However, since one can of course never be completely sure of the specificity of a pharmacological tool, we would like to acknowledge here that there were some differences in the brain cytokine profiles between the KCa3.1<sup>-/-</sup> mice and the TRAM-34 treated wild-type animals that could suggest possible off-target effects of the drug or compensation effects in the knockout mice. It therefore would be desirable to repeat this study in an inducible, tissue specific knockout animal.

Another question is of course whether KCa3.1 inhibition, which we and others have previously proposed for the treatment of asthma,<sup>34</sup> inflammatory bowel disease<sup>35</sup> and transplant vasculopathy<sup>22</sup> will increase the risk of infections. In this context it should be kept in mind that the interactions between the brain and the immune system during and after stroke are complex. While splenectomy in rats<sup>36</sup> or T cell deficiency in mice<sup>37</sup> results in smaller infarcts and improved functional outcomes, clinical experience shows that stroke induces a state of immunodepression putting the patient at increased risk of respiratory and urinary tract infections, which are responsible for considerable morbidity and mortality after stroke. This phenomenon is considered to be mediated by hyperactivity of the sympathetic nervous system and increased release of cortisol and catecholamines. We do not believe that KCa3.1 inhibition will increase the risk of post-stroke infections because KCa3.1 blockers are relatively “mild” immunosuppressants that

do not reduce the ability of rodents to clear viral infections.<sup>38</sup> Pharmacological KCa3.1 blockade further seems to be generally safe. Daily administration of TRAM-34 at 120 mg/kg/d for six months did not induce any signs of toxicity in rats,<sup>14</sup> while Senicapoc, a KCa3.1 blocker structurally very similar to our TRAM-34, advanced up to Phase-3 clinical trials for sickle cell anemia,<sup>39</sup> where it failed for lack of efficacy in reducing the number of painful sickling crisis and not because of toxicity issues or an increased risk of infections. Senicapoc was subsequently deposited by Pfizer in the NCATs library and would theoretically be available for investigator-initiated clinical trials.

In conclusion, we are proposing KCa3.1 blockers as an alternative to minocycline for reducing microglia/macrophage activation in the first week after ischemic stroke. The 12-hour window of opportunity makes KCa3.1 blocker particularly attractive in our opinion. The next step in evaluation KCa3.1 blockers for stroke therapy will of course have to be a direct comparison with minocycline in a setting where both compounds are optimally dosed in order to determine if KCa3.1 inhibitors offer any advantages.

## **DISCLOSURE/CONFLICT OF INTEREST**

H.W. is an inventor on a University of California patent claiming TRAM-34 and related triarylmethanes for immunosuppression. This patent has recently been abandoned by the University of California because it issued in 2000 and is close to expiring.

## **AUTHOR CONTRIBUTIONS**

YC, HMN, IM, LWJ and HW conceptualized and designed the study. YC, HMN, IM and HW undertook experiments, analyzed data, prepared figures and wrote the paper. RK provided the *KCa3.1<sup>-/-</sup>* mice and critically participated in the writing. ALG and EMG performed behavioral or immunohistochemical experiments. All authors critically reviewed the manuscript and approved the final manuscript as submitted and agree to be accountable for all aspects of the work.

**REFERENCES**

1. Nimmerjahn A, Kirchhoff F, Helmchen F. Resting microglial cells are highly dynamic surveillants of brain parenchyma in vivo. *Science*. 2005; **308**: 1314-1318.
2. Macrez R, Ali C, Toutirais O, Le Mauff B, Defer G, Dirnagl U, et al. Stroke and the immune system: From pathophysiology to new therapeutic strategies. *Lancet Neurol* 2011; **10**: 471-480.
3. Iadecola C, Anrather J. The immunology of stroke: From mechanisms to translation. *Nat Med* 2011; **17**: 796-808.
4. Kawabori M, Yenari MA. The role of the microglia in acute cns injury. *Metab Brain Dis* 2015; **30**: 381-392.
5. Prinz M, Priller J, Sisodia SS, Ransohoff RM. Heterogeneity of cns myeloid cells and their roles in neurodegeneration. *Nat Neurosci* 2011; **14**: 1227-1235.
6. Turner RC, Dodson SC, Rosen CL, Huber JD. The science of cerebral ischemia and the quest for neuroprotection: Navigating past failure to future success. *J Neurosurg* 2013; **118**: 1072-1085.
7. Fagan SC, Cronic LE, Hess DC. Minocycline development for acute ischemic stroke. *Transl Stroke Res* 2011; **2**: 202-208.
8. Lampl Y, Boaz M, Gilad R, Lorberboym M, Dabby R, Rapoport A, et al. Minocycline treatment in acute stroke: An open-label, evaluator-blinded study. *Neurology* 2007; **69**: 1404-1410.
9. Fordyce CB, Jagasia R, Zhu X, Schlichter LC. Microglia Kv1.3 channels contribute to their ability to kill neurons. *J Neurosci* 2005; **25**: 7139-7149.

10. Kaushal V, Koeberle PD, Wang Y, Schlichter LC. The Ca<sup>2+</sup>-activated K<sup>+</sup> channel KCNN4/KCa3.1 contributes to microglia activation and nitric oxide-dependent neurodegeneration. *J Neurosci* 2007; **27**: 234-244.
11. Maezawa I, Zimin P, Wulff H, Jin LW. A-beta oligomer at low nanomolar concentrations activates microglia and induces microglial neurotoxicity. *J Biol Chem* 2011; **286**: 3693-3706.
12. Feske S, Wulff H, Skolnik EY. Ion channels in innate and adaptive immunity. *Ann Rev Immunol* 2015; **33**: 291-353.
13. Kettenmann H, Hanisch UK, Noda M, Verkhratsky A. Physiology of microglia. *Physiol Rev* 2011; **91**: 461-553.
14. Chen YJ, Raman G, Bodendiek S, O'Donnell ME, Wulff H. The KCa3.1 blocker TRAM-34 reduces infarction and neurological deficit in a rat model of ischemia/reperfusion stroke. *J Cereb Blood Flow Metab* 2011; **31**: 2363 – 2374.
15. Si H, Heyken WT, Wolfle SE, Tysiac M, Schubert R, Grgic I, et al. Impaired endothelium-derived hyperpolarizing factor-mediated dilations and increased blood pressure in mice deficient of the intermediate-conductance Ca<sup>2+</sup>-activated K<sup>+</sup> channel. *Circ Res* 2006; **99**: 537-544.
16. Longa EZ, Weinstein PR, Carlson S, Cummins R. Reversible middle cerebral artery occlusion without craniectomy in rats. *Stroke* 1989; **20**: 84-91.
17. Wulff H, Miller MJ, Haensel W, Grissmer S, Cahalan MD, Chandy KG. Design of a potent and selective inhibitor of the intermediate-conductance Ca<sup>2+</sup>-activated K<sup>+</sup> channel, IKCa1: A potential immunosuppressant. *Proc Natl Acad Sci USA* 2000; **97**: 8151-8156.

18. Menzies SA, Hoff JT, Betz AL. Middle cerebral artery occlusion in rats: A neurological and pathological evaluation of a reproducible model. *Neurosurgery* 1992; **31**: 100-106.
19. De Ryck M, Van Reempts J, Borgers M, Wauquier A, Janssen PA. Photochemical stroke model: Flunarizine prevents sensorimotor deficits after neocortical infarcts in rats. *Stroke* 1989; **20**: 1383-1390.
20. Wulff H, Calabresi PA, Allie R, Yun S, Pennington M, Beeton C, et al. The voltage-gated Kv1.3 K<sup>+</sup> channel in effector memory T cells as new target for MS. *J Clin Invest* 2003; **111**: 1703-1713.
21. Schmitz A, Sankaranarayanan A, Azam P, Schmidt-Lassen K, Homerick D, Hansel W, et al. Design of PAP-1, a selective small molecule Kv1.3 blocker, for the suppression of effector memory T cells in autoimmune diseases. *Mol Pharmacol* 2005; **68**: 1254-1270.
22. Chen YJ, Lam J, Gregory CR, Schrepfer S, Wulff H. The Ca<sup>2+</sup>-activated K<sup>+</sup> channel KCa3.1 as a potential new target for the prevention of allograft vasculopathy. *PLoS ONE*. 2013; **8**: e81006.
23. Fox C, Dingman A, Derugin N, Wendland MF, Manabat C, Ji S, et al. Minocycline confers early but transient protection in the immature brain following focal cerebral ischemia-reperfusion. *J Cereb Blood Flow Metab* 2005; **25**: 1138-1149.
24. Maezawa I, Nivison M, Montine KS, Maeda N, Montine TJ. Neurotoxicity from innate immune response is greatest with targeted replacement of E4 allele of apolipoprotein E gene and is mediated by microglial p38MAPK. *FASEB J* 2006; **20**: 797-799.
25. Schlattmann P, Dirnagl U. Statistics in experimental cerebrovascular research: Comparison of more than two groups with a continuous outcome variable. *J Cereb Blood Flow Metab* 2010; **30**: 1558-1563.

26. McNeish AJ, Sandow SL, Neylon CB, Chen MX, Dora KA, Garland CJ. Evidence for involvement of both IKCa and SKCa channels in hyperpolarizing responses of the rat middle cerebral artery. *Stroke* 2006; **37**: 1277-1282.
27. Rus H, Pardo CA, Hu L, Darrah E, Cudrici C, Niculescu T, et al. The voltage-gated potassium channel Kv1.3 is highly expressed on inflammatory infiltrates in multiple sclerosis brain. *Proc Natl Acad Sci U S A* 2005; **102**: 11094-11099.
28. Zaritsky JJ, Eckman DM, Wellman GC, Nelson MT, Schwarz TL. Targeted disruption of Kir2.1 and Kir2.2 genes reveals the essential role of the inwardly rectifying K<sup>+</sup> current in K<sup>+</sup>-mediated vasodilation. *Circ Res* 2000; **87**: 160-166.
29. Boucsein C, Kettenmann H, Nolte C. Electrophysiological properties of microglial cells in normal and pathologic rat brain slices. *Eur J Neurosci.* 2000; **12**: 2049-2058.
30. Lyons SA, Pastor A, Ohlemeyer C, Kann O, Wiegand F, Prass K, et al. Distinct physiologic properties of microglia and blood-borne cells in rat brain slices after permanent middle cerebral artery occlusion. *J Cereb Blood Flow Metab* 2000; **20**: 1537-1549.
31. King B, Rizwan AP, Asmara H, Heath NC, Engbers JD, Dykstra S, et al. IKCa channels are a critical determinant of the slow ahp in cal pyramidal neurons. *Cell Rep* 2015; **11**: 175-182.
32. Yenari MA, Kauppinen TM, Swanson RA. Microglial activation in stroke: Therapeutic targets. *Neurotherapeutics* 2010; **7**: 378-391.
33. Chen YJ, Wallace BK, Yuen N, Jenkins DP, Wulff H, O'Donnell ME. Blood-brain barrier KCa3.1 channels: Evidence for a role in brain Na uptake and edema in ischemic stroke. *Stroke* 2015; **46**: 237-244.

34. Girodet PO, Ozier A, Carvalho G, Ilina O, Ousova O, Gadeau AP, et al. Ca<sup>2+</sup>-activated K<sup>+</sup> channel-3.1 blocker TRAM-34 attenuates airway remodeling and eosinophilia in a murine asthma model. *Am J Respir Cell Mol Biol* 2013; **48**: 212-219.
35. Di L, Srivastava S, Zhdanova O, Ding Y, Li Z, Wulff H, et al. Inhibition of the K<sup>+</sup> channel KCa3.1 ameliorates T cell-mediated colitis. *Proc Natl Acad Sci USA* 2010; **107**: 1541-1546.
36. Ajmo CT, Jr., Vernon DO, Collier L, Hall AA, Garbuzova-Davis S, Willing A, et al. The spleen contributes to stroke-induced neurodegeneration. *J Neurosci Res* 2008; **86**: 2227-2234.
37. Yilmaz G, Arumugam TV, Stokes KY, Granger DN. Role of T lymphocytes and interferon-gamma in ischemic stroke. *Circulation* 2006; **113**: 2105-2112.
38. Toyama K, Wulff H, Chandy KG, Azam P, Raman G, Saito T, et al. The intermediate-conductance calcium-activated potassium channel KCa3.1 contributes to atherogenesis in mice and humans. *J Clin Invest* 2008; **118**: 3025-3037.
39. Ataga KI, Reid M, Ballas SK, Yasin Z, Bigelow C, James LS, et al. Improvements in haemolysis and indicators of erythrocyte survival do not correlate with acute vaso-occlusive crises in patients with sickle cell disease: A phase III randomized, placebo-controlled, double-blind study of the gardos channel blocker senicapoc (ICA-17043). *Br J Haematol* 2011; **153**: 92-104.

**FIGURE LEGENDS**

**Figure 1.** Scheme illustrating isolation of microglia for confocal microscopy and electrophysiological experiments with CD11b<sup>+</sup> magnetic beads from the infarct area 8 days after MCAO.

**Figure 2.** K<sup>+</sup> channel expression in acutely isolated microglia. **(A)** Kv1.3 current density increases in microglia from the infarct area after MCAO ( $28.8 \pm 2.0$  pA/pF, n = 19) and microglia isolated from the hippocampus following intracerebroventricular LPS injection ( $22.9 \pm 16.6$  pA/pF, n = 13) compared to microglia from wild-type control brains ( $5.0 \pm 3.9$  pA/pF, n = 16) or microglia from the contralateral side after MCAO ( $5.7 \pm 4.4$  pA/pF, n = 18). **(B)** Example current traces showing Kv1.3's characteristic use-dependence and sensitivity to the Kv1.3 blockers PAP-1 and ShK-L5. **(C)** Microglia from the contralateral ( $50.2 \pm 35.4$  pS/pF, n = 18) and ipsilateral side after MCAO ( $71.6 \pm 34.9$  pS/pF, n = 21), as well as microglia isolated from the hippocampus following intracerebroventricular LPS injection ( $84.0 \pm 42.4$  pS/pF, n = 13) show higher KCa3.1 current densities than microglia from wild-type control brains ( $29.7 \pm 15.2$  pS/pF, n = 16). **(D)** Example KCa3.1 current traces elicited by a ramp protocol showing the current's sensitive to 1  $\mu$ M of the KCa3.1-selective blocker TRAM-34. **(E)** Microglia from both the contralateral side ( $7.8 \pm 5.8$  pA/pF, n = 18) and the infarct area ( $15.1 \pm 10.2$  pA/pF, n = 21) after MCAO show increased Kir current densities compared to those from wild-type ( $2.4 \pm 2.4$  pA/pF, n = 16) or LPS-injected brains ( $1.9 \pm 2.9$  pA/pF, n = 13). **(F)** Representative current traces showing a large Kir current, which was observable in some MCAO microglia, but not in microglia isolated from the hippocampus following intracerebroventricular LPS injection. Data are presented as mean  $\pm$  S.D. Statistical significance was determined by Student's *t*-test.

**Figure 3.** KCa3.1 and Kv1.3 are expressed on microglia/macrophages in human infarcts. **(A)** KCa3.1 staining in a 2-3-week old infarct. KCa3.1 expression is localized to macrophages/microglia (M) and

vascular endothelial (E) cells. **(B)** Fluorescent staining for a microglia/macrophage marker (MAC387) and KCa3.1. **(C)** Kv1.3 staining in a 14-day old infarct. **(D)** Fluorescent staining for a microglia/macrophage marker (MAC387) and Kv1.3. All images are from 5- $\mu$ m thick paraffin sections.

**Figure 4.** KCa3.1 expression on microglia/macrophages in mouse infarcts. **(A)** Fluorescent staining for KCa3.1 and CD68 in the infarct area of *KCa3.1<sup>-/-</sup>* **(A)** and wild-type **(B)** mice five days after MCAO with reperfusion. **(C)** Higher magnification image showing that KCa3.1 and CD68 do not colocalize. All panels are confocal images from 5- $\mu$ m thick paraffin sections.

**Figure 5.** Genetic KCa3.1 deletion and pharmacological blockade with TRAM-34 reduce infarction and improve neurological deficit. **(A)** NeuN-defined infarct area in mice subjected to 60 min of MCAO followed by 8 days of reperfusion in brain slices 2, 4, 6, and 8 mm from the frontal pole. Shown are vehicle-treated wild-type mice (n = 11), vehicle-treated *KCa3.1<sup>-/-</sup>* mice (n = 17) and wild-type mice treated with TRAM-34 at 40 mg/kg twice daily starting 12 hours after reperfusion (n = 11). \**p* <0.05, \*\**p* <0.01, \*\*\**p* <0.001. **(B)** Neurological deficit in the 4-score system (normal mouse = 0). **(C)** Neurological deficit in the 14-score system (normal mouse = 14). \**p* <0.05, #*p* <0.01, &*p* <0.001. All values in panels A, B and C are mean  $\pm$  S.E.M.

**Figure 6.** Genetic KCa3.1 deletion and pharmacological blockade with TRAM-34 reduce microglia activation and cytokine production. **(A)** Microglia/macrophage activation/proliferation/infiltration as determined by the ratio of the Iba-1-positive cells in the ipsi- versus contralateral hemisphere from the 4- and 6-mm slices from all animals in vehicle treated wild-type mice (n = 11), vehicle treated *KCa3.1<sup>-/-</sup>* mice (n = 17) and wild-type mice treated with TRAM-34 at 40 mg/kg twice daily starting 12 hours after reperfusion (n = 11). **(B)** Brain cytokine concentrations in the ipsi- and contralateral side 8 days after MCAO from vehicle treated wild-type mice, *KCa3.1<sup>-/-</sup>* mice, TRAM-34 treated wild-type mice and

vehicle treated sham operated wild-type mice (n = 3 in every case). \* $p < 0.05$ , \*\* $p < 0.01$ . Values are mean  $\pm$  S.E.M.

**Figure 7.** TRAM-34 reduces microglia activation and neuronal death in organotypic hippocampal slices. **(A)** Hippocampal slices were subjected to 60 min of hypoxia and hypoglycemia and stained for Iba-1 (green) to evaluate microglia activation and NeuN (red) to evaluate neurotoxicity 3 days later. TRAM-34 and doxycycline were added 2 h after the end of the hypoxia. **(B)** Quantification of data shown in A from 5 slices. The number of Iba-1 and NeuN positive cells were counted using ImageJ software and normalized by the total number of DAPI positive cells. **(C)** Hypoxia induced IL-1 $\beta$  production measured in the medium of the slice culture on day-3 (n = 4). Shown are means  $\pm$  S.E.M. Statistical analyses were performed using SigmaPlot 11 software (Systat Software, Inc.). Analysis of variance or repeated-measures analysis of variance was used to compare quantitative values from cultures across groups. Tukey's studentized range test was used to adjust for multiple comparisons in post hoc pairwise tests.

## Isolation of Ischemia-activated microglia (CD11b magnetic micro-beads)

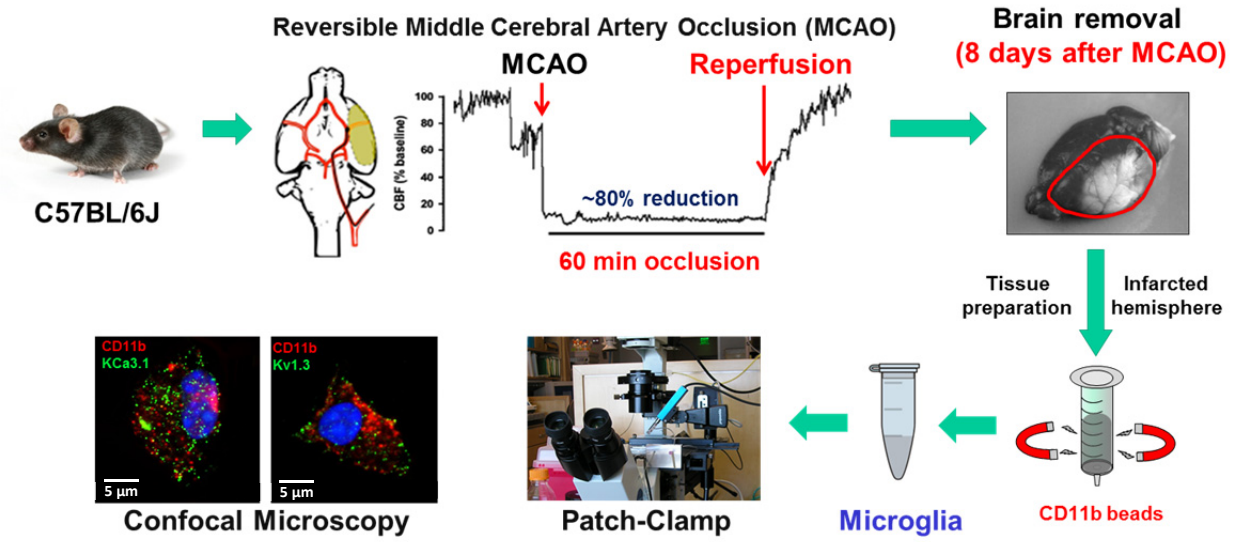


Figure 1

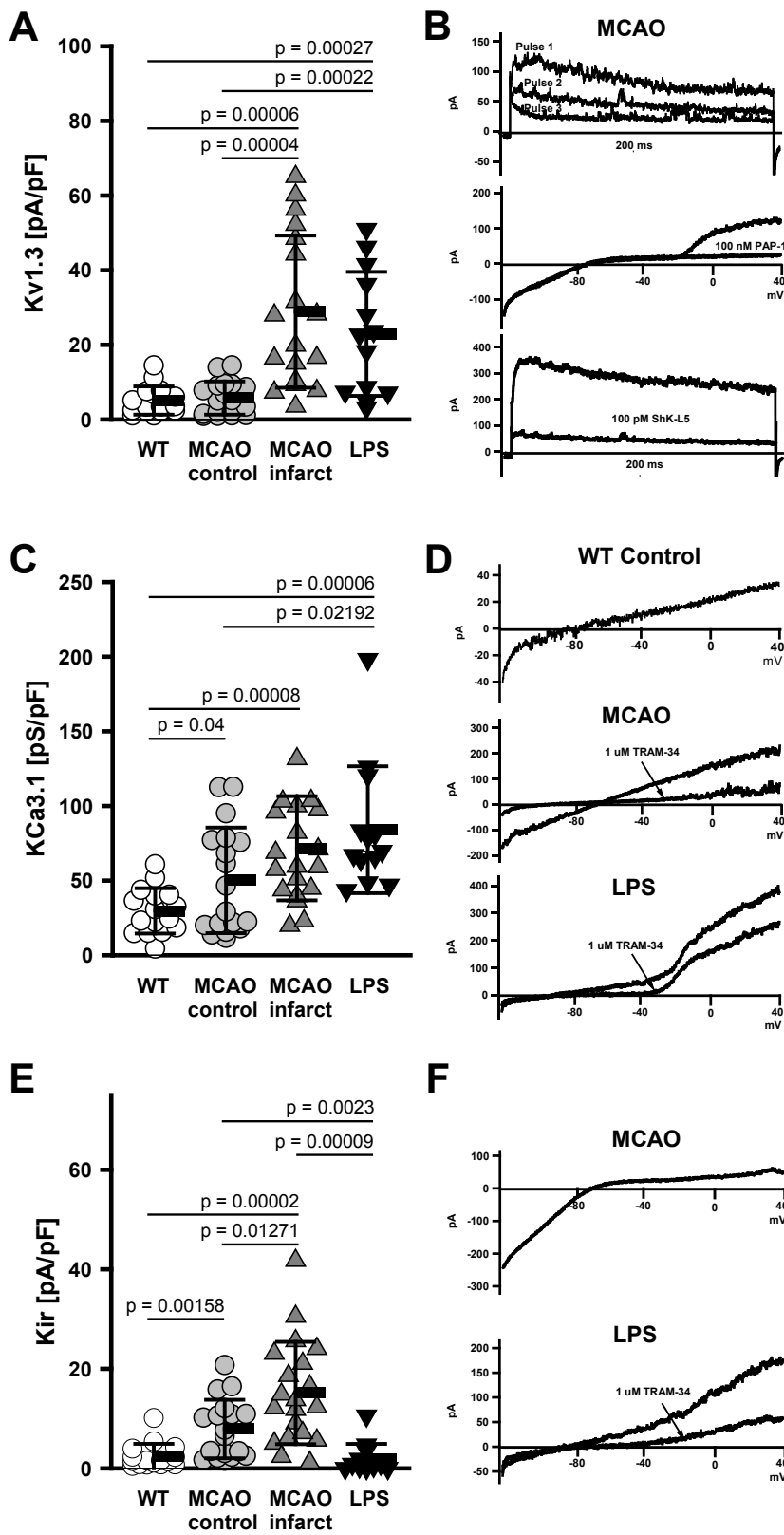
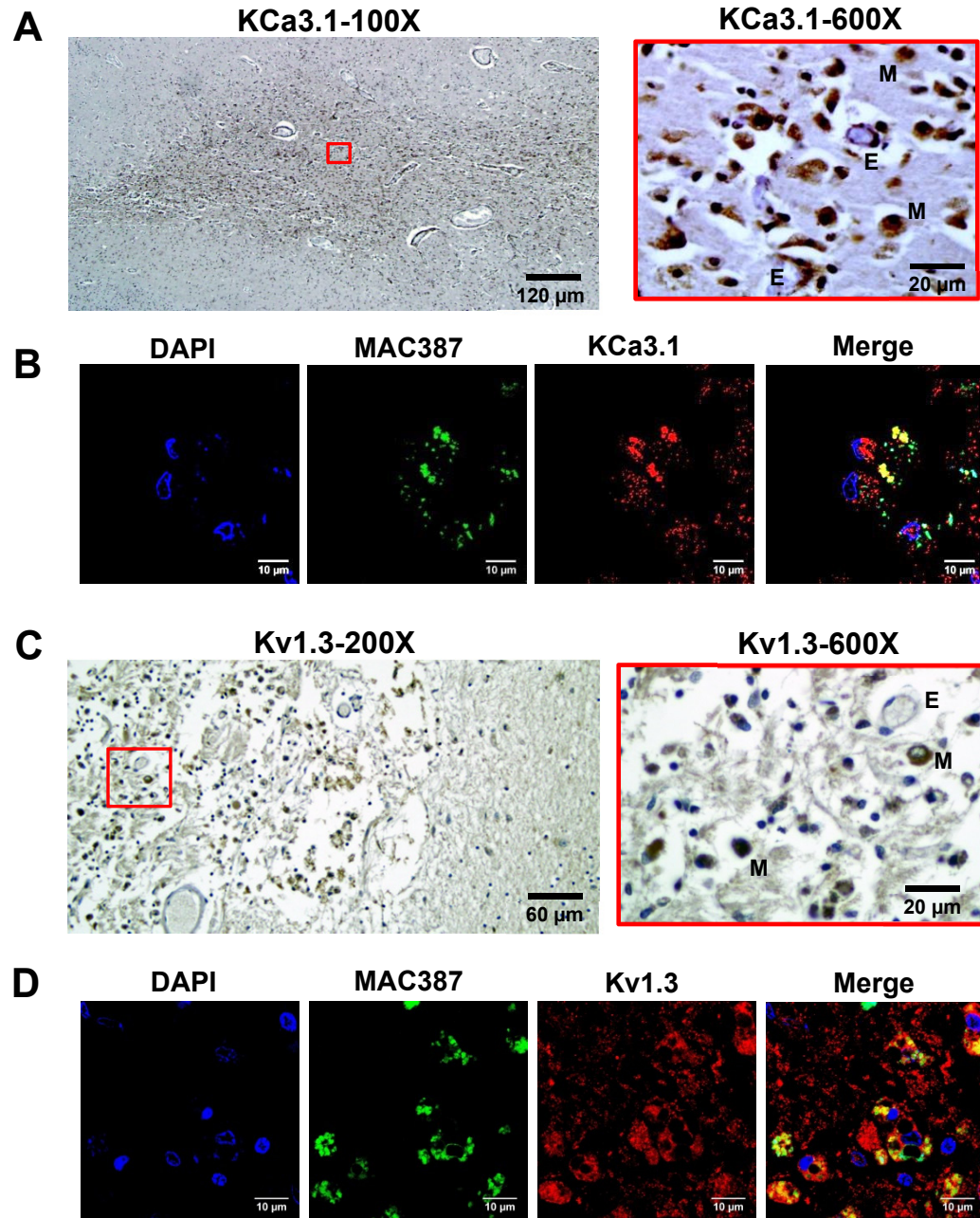
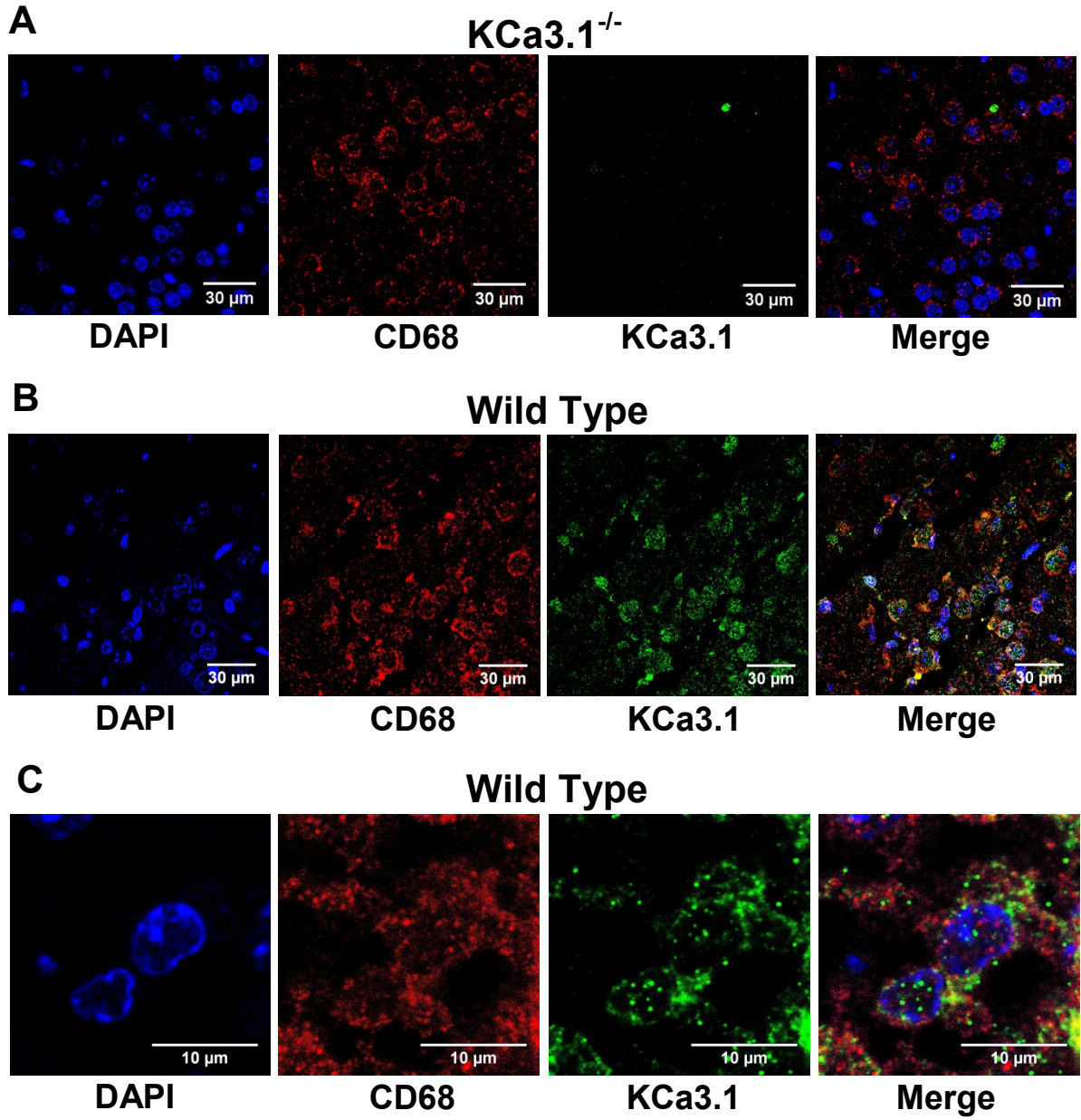
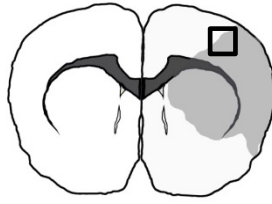


Figure 2



**Figure 3**



**Figure 4**

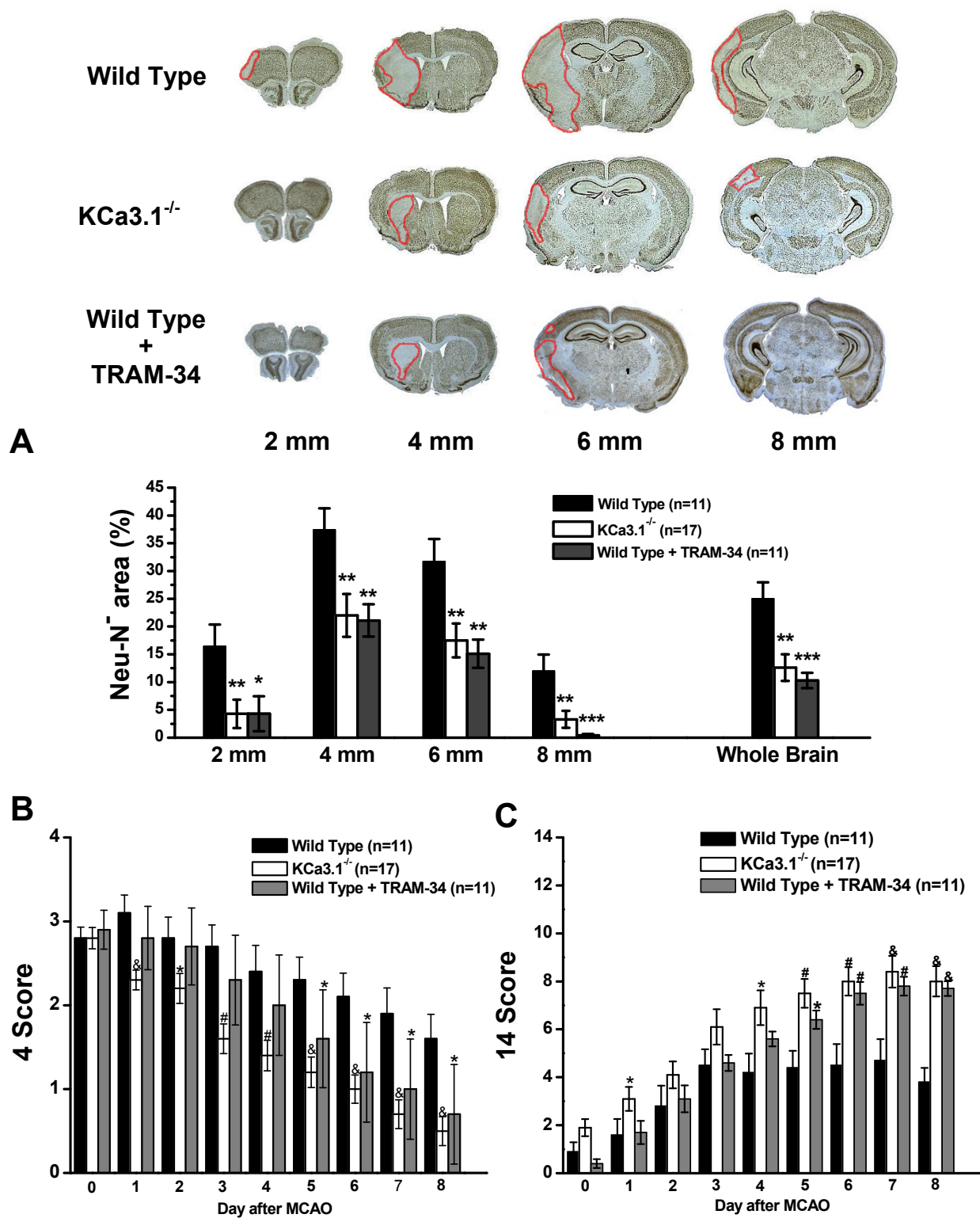
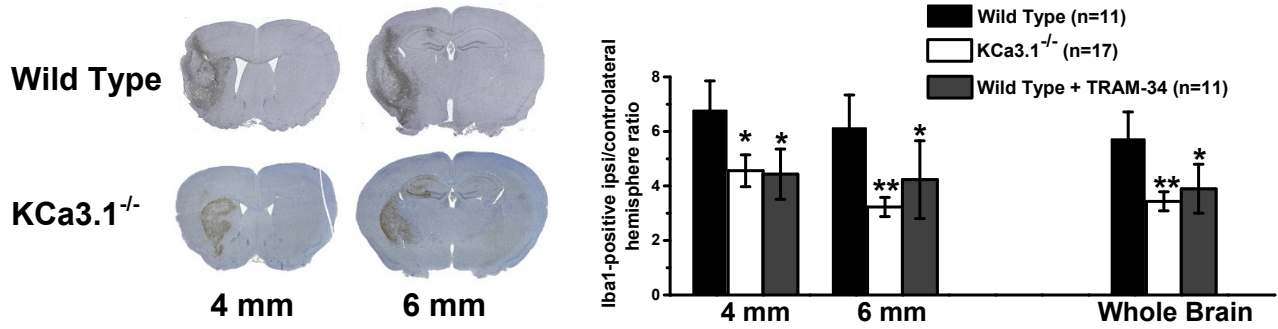
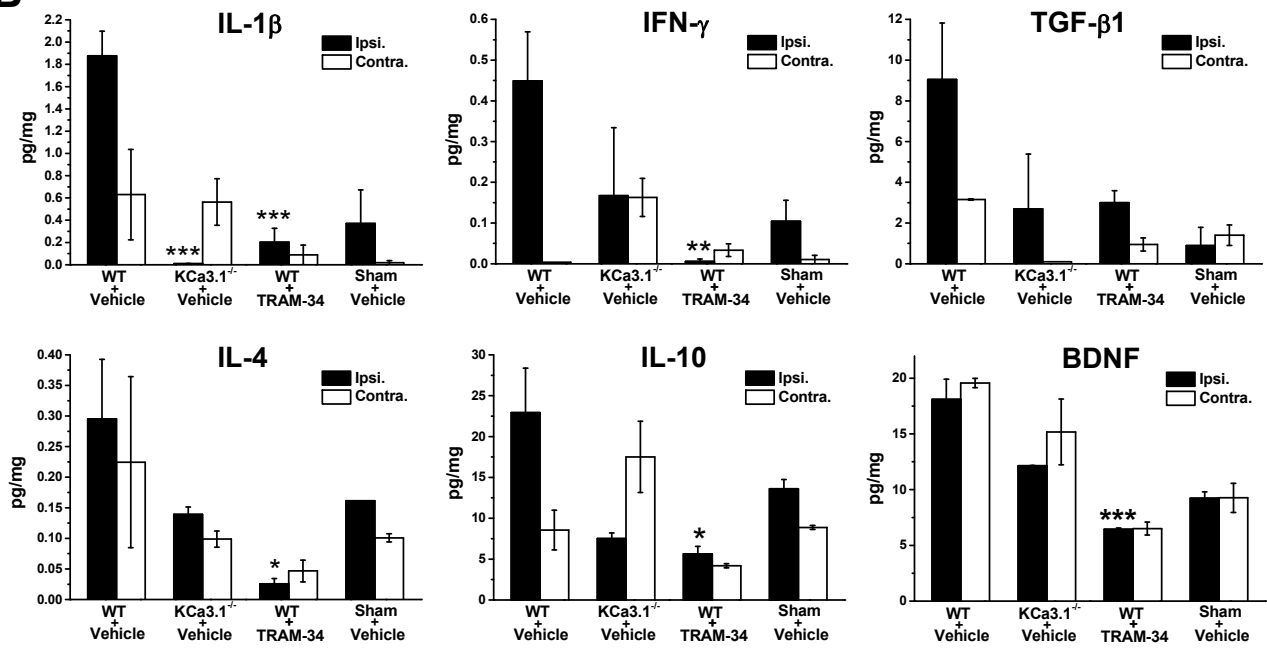


Figure 5

**A**



**B**



**Figure 6**

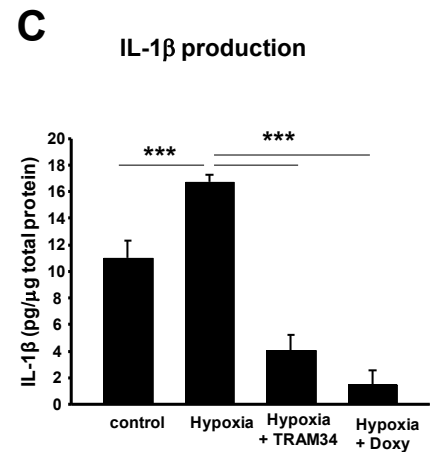
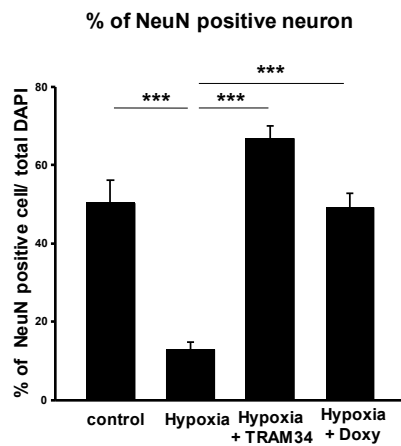
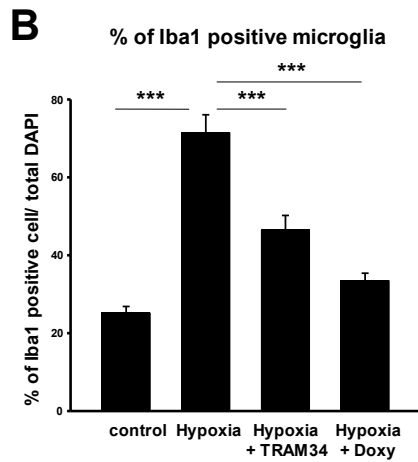
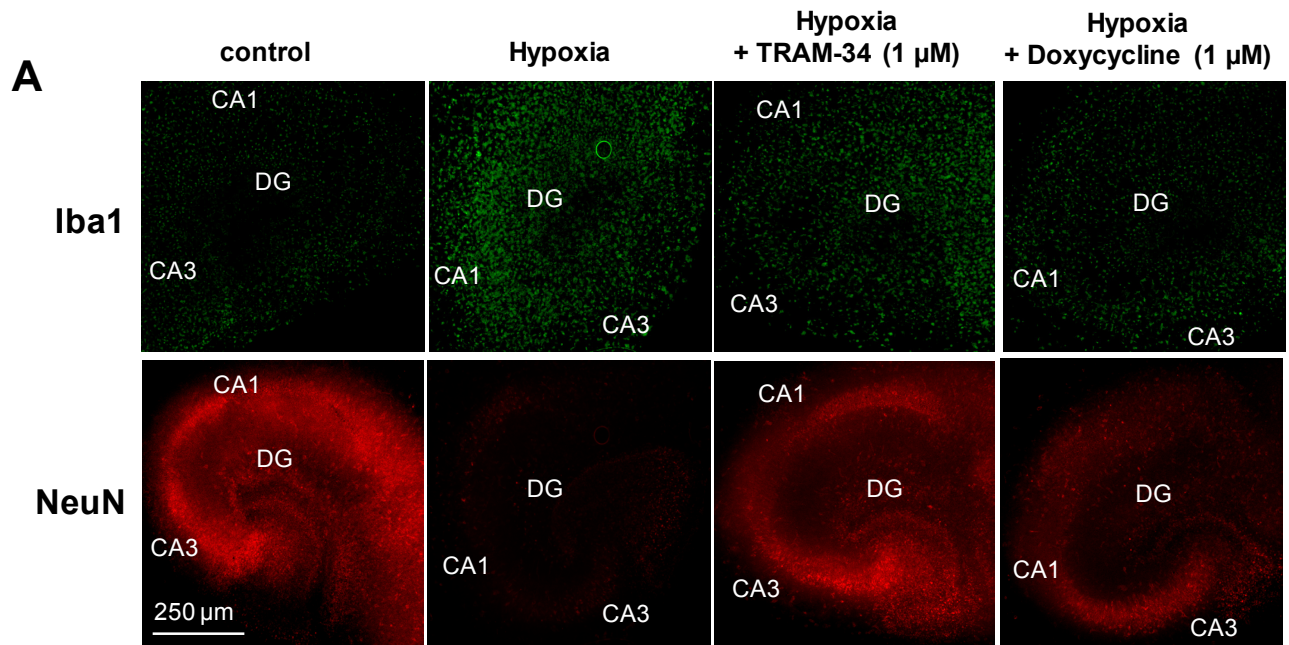


**Figure 7**